

摆动 TIG 焊搭接坡口数学建模与仿真

洪 波, 黄明灿, 尹 力, 龚 海

(湘潭大学 机械工程学院, 湖南 湘潭 411105)



洪 波

摘 要: 针对搭接坡口的特点, 在摆动 TIG 焊搭接坡口电弧扫描的数学模型中采用电弧圆柱体体积的变化信号作为系统的输入信号, 从而建立了系统的整体仿真模型。在保证工艺参数不变的情况下, 比较分析了该模型的仿真结果与传统的利用焊枪高度变化为输入的模型的仿真结果以及实际的焊接波形之间的差异。结果表明, 仿真结果与试验结果相吻合, 证明该模型比传统的模型更为精确, 更能反映实际情况。对搭接坡口的焊缝跟踪系统研究有一定的指导意义。

关键词: 钨极惰性气体保护焊; 搭接坡口; 数学建模仿真; 电弧圆柱体

中图分类号: TG115.28 **文献标识码:** A **文章编号:** 0253-360X(2008)07-0043-04

0 序 言

钨极氩弧焊是以钨材料或钨的合金材料做电极, 在惰性气体保护下进行的焊接, 在钨电极的周围通过喷嘴送进保护气, 保护钨电极、电弧及熔池, 使其免受大气的侵害^[1], 几乎可用于所有钢材、有色金属及其合金的焊接。目前对于 TIG 焊自动跟踪方面的研究随着计算机仿真技术的迅速发展, 对于焊缝跟踪的仿真已经在各种焊接方法中实现, 但中国 TIG 焊自动跟踪方面的研究略显不足, 文中以 TIG 焊焊接中常见的搭接坡口为例, 利用 MATLAB 软件建立 TIG 焊摆动电弧扫描系统仿真模型, 进行仿真分析。

美国 Bient K Christer 等人^[2] 1998 年的研究表明, 电弧长度与电弧电压之间为典型的线性关系, 传统的建模都利用这一原理。利用这个原理在搭接坡口扫描时, 焊枪高度(电弧长度)的变化是非线性的, 但是在实际焊接过程中, 电弧电压是一个线性变化的量。为了弥补这一缺陷, 在仿真模型中, 通过合理的假设, 建立电弧圆柱体体积与电弧电压之间的关系。电弧的横截面积主要与焊接电流的大小有关, 受电压的影响比较小, 由 TIG 焊的恒流特性, 假设在一定的焊接工艺参数条件下电弧横截面积是恒定值, 电弧长度乘以一个横截面积常量得到电弧圆柱体体积, 因此, 电弧圆柱体体积与电弧电压之间

也是典型的线性关系。由电弧圆柱体体积的变化, 利用体积与电压之间的转换系数 K 得到电弧电压的变化波形, 文中在此原理基础上利用 MATLAB^[3,4] 建立 TIG 焊搭接坡口数值仿真模型, 并且通过此模型的仿真结果与传统建模方法的仿真结果, 以及实际焊接波形三者之间的比较, 验证了模型的可靠性和优越性。

1 数值仿真模型的建立

1.1 电弧扫描搭接坡口体积变化规律

该模型建立电弧扫描过程中电弧圆柱体体积变化与时间之间的关系, 由于斜切焊炬圆柱体体积计算比较复杂, 而摆动幅度与摆动臂长之比很小, 为了研究的方便, 做如下几个假设。

(1) 焊接电弧为圆柱体, 在一定的焊接工艺参数条件下, 焊接电流恒定不变, 电弧横截面积只受焊接电流的影响, 也是恒定值。又因为电弧长度与电弧电压存在线性关系, 所以在一定的焊接工艺参数条件下, 电弧电压与电弧圆柱体体积成正比。

(2) 电弧圆柱体在扫描过程中始终为竖直方向放置。

(3) 电弧圆柱体在扫描过程中移动方向始终为水平方向, 而且速度均匀平稳。

(4) 忽略了坡口熔化以及其它的一些因素的影响。

图 1 给出了搭接坡口电弧扫描的示意图以及部分符号的物理意义。

收稿日期: 2007-08-01

基金项目: 湖南省教育厅资助项目(06A073); 湘潭大学交叉项目(06IND05)

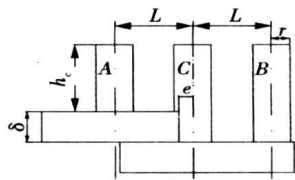


图 1 搭接坡口电弧扫描的示意图
Fig 1 Arc scanning for lap joint groove

$$V(t) = \begin{cases} h\pi r^2, & 0 \leq t < t_1 \\ h\pi r^2 - \delta \left[\frac{1}{2}\pi r^2 - r^2 \arcsin\left(\frac{L}{r} + \frac{e}{r} - \frac{4L}{Tr}t\right) - (L + e - \frac{4L}{T}t) \times \right. \\ \quad \left. \sqrt{(r + L + e - \frac{4L}{T}t)(r - L - e + \frac{4L}{T}t)} \right], & t_1 \leq t < t_2 \\ (h_c - \delta\pi r^2, & t_2 \leq t < t_3 \\ (h_c - \delta\pi r^2 + \delta \left[\frac{1}{2}\pi r^2 - r^2 \arcsin\left(\frac{3L}{r} - \frac{e}{r} - \frac{4L}{Tr}t\right) - (3L - e - \frac{4L}{T}t) \times \right. \\ \quad \left. \sqrt{(r + 3L - e - \frac{4L}{T}t)(r - 3L + e + \frac{4L}{T}t)} \right], & t_3 \leq t < t_4 \\ h\pi r^2, & t_4 \leq t < T \end{cases}$$

式中: $t_1 = (\frac{T}{4}) + \frac{[0.25(e-r)T]}{L}$;
 $t_2 = (\frac{T}{4}) + \frac{[0.25(e+r)T]}{L}$;
 $t_3 = (\frac{T}{2}) + \frac{[0.25(L-e-r)T]}{L}$;
 $t_4 = (\frac{T}{2}) + \frac{[0.25(L-e+r)T]}{L}$;

式中: h_c 为电弧圆柱体的高度; δ 为上搭板厚度; e 为焊枪对中偏差; r 为电弧圆柱体底面半径; T 为摆动周期。

1.2 摆动 TIG 焊搭接坡口数学模型的建立

$V(t)$ 是焊接电弧在扫描搭接坡口时体积随时间的变化规律, 由序言介绍可以知道体积与电压存在线性关系: $U(t) = KV(t)$, 其中 K 为比例系数, 由此建立搭接坡口电弧扫描的 MATLAB 仿真模型, 如图 2 所示。

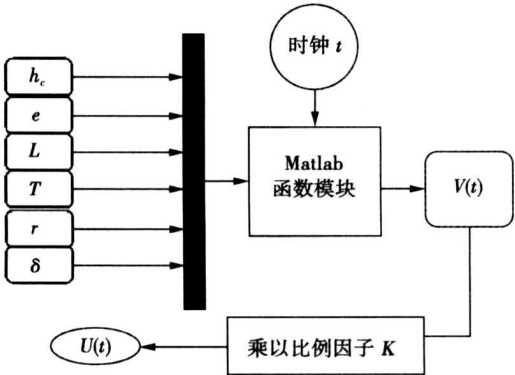


图 2 系统 MATLAB 仿真模型
Fig 2 MATLAB modeling

其中, C 为电弧圆柱体摆动中心位置, B 为电弧圆柱体摆动到最右端位置, A 为电弧圆柱体摆动到最左端位置。为分析方便假设电弧圆柱体摆动到坡口的最右侧时, $t=0$, 对搭接坡口, 在电弧圆柱体偏离焊缝中心 e ($-L \leq e \leq L$, 其中 L 为距摆动中心的位移) 的情况下, 在一个摆动周期 ($0 \leq t \leq T$) 内电弧圆柱体体积变化为

图 3 是系统模型的数据处理流程图。主要分为四个步骤: 第一步, 初始化系统, 由输入的参数确定函数中常数的取值; 第二步, 对时间 t 进行处理, 确定其在一个周期内所处的区间; 第三步, 根据 t 所在的区间, 调用程序计算 $V(t)$ 的值; 第四步, 利用 $V(t)$ 与 $U(t)$ 转化的比例系数 K 求得得到电弧电压

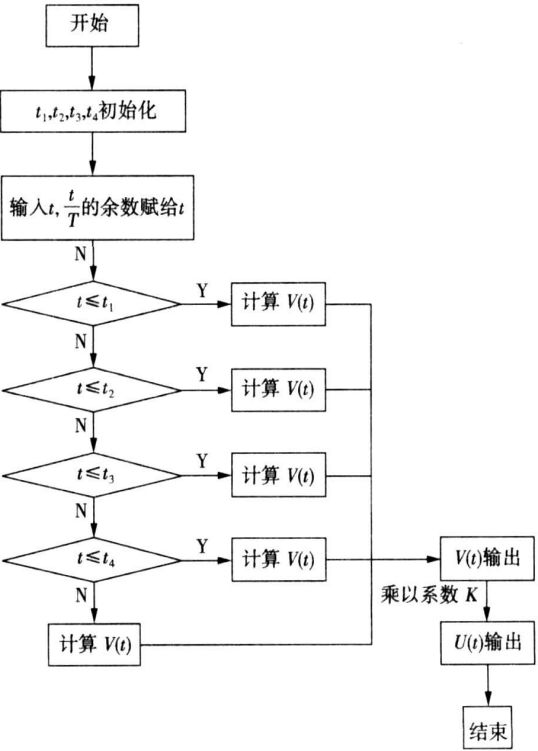


图 3 系统流程图
Fig 3 System schematic diagram

$U(t)$ 。

2 仿真分析与讨论

2.1 电压波形仿真结果

由前面建立的整体仿真模型, 选定参数进行数值计算, 得到部分的输出结果。图 4 是电弧扫描电压输出 U_s 的变化仿真波形。

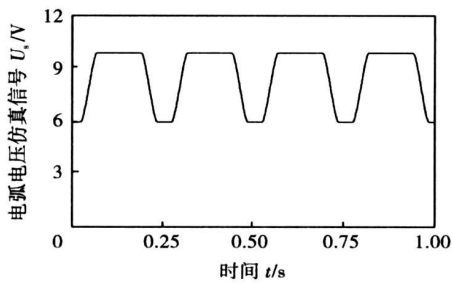


图 4 搭接坡口电压变化仿真波形
Fig 4 Simulated result of voltage signal

仿真参数: $h_c=3\text{ mm}$, $\delta=2\text{ mm}$, $e=1\text{ mm}$, $L=3\text{ mm}$, $r=1\text{ mm}$, $T=0.25\text{ s}$, 采用传统的焊枪高度变化扫描的建模方法, 得到的仿真结果(见图 5)。

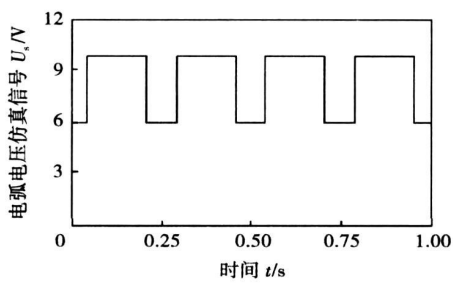


图 5 传统模型系统电压变化仿真波形
Fig. 5 Simulated result of voltage signal for trational model

比较两种模型得到的电压仿真信号, 可以发现, 传统模型仿真结果中, 当电弧扫描通过搭接坡口的时候, 电压有一个阶越变化, 而文中所建立的建模仿真结果中, 过渡比较缓和。

2.2 仿真结果的试验验证

为了比较两种模型之间的优劣, 采用与仿真计算过程类似的工艺参数进行了焊接试验, 试验采用的焊接电源是垂直陡降特性直流模拟式焊接电源(PANA-TIG WP300), 钨极直径为 $\phi 1.2\text{ mm}$, 钨极尖端锥度为 20° , 氩气流量为 5 ml/s , 摆动频率为 4 Hz ,

对中偏差为 1 mm , 摆动幅度为 3 mm 。得到的电弧电压采样波形如图 6 中所示。图 7 为焊缝实物图。

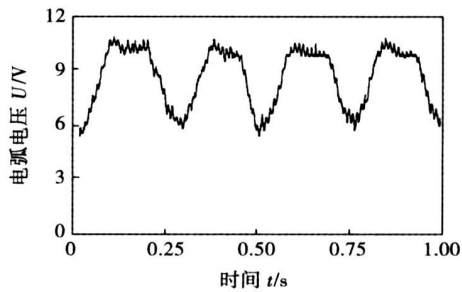


图 6 实际电弧电压波形
Fig 6 Experimental results of welding voltage

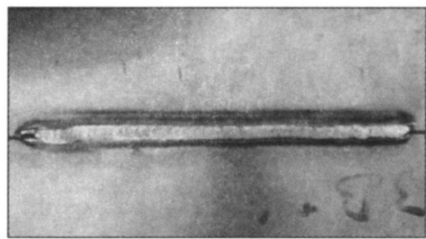


图 7 焊缝实物图
Fig. 7 Welded joint image

比较由三种方法得到的电压变化信号, 可以发现, 在电弧电压总体变化趋势上, 前面两个模型得到的结果与图 6 中实际电弧电压波形的变化是一致的。但也有区别, 实际电弧电压在上升和下降阶段基本对称, 且都是有一定的斜率, 这与文中所建立的模型相当吻合, 而传统模型得到的波形的上升和下降都是垂直变化的, 与实际波形相差较远。

前面做的是焊接对中偏差 $e=1\text{ mm}$ 的情况, 此外还考虑了对中偏差 $e=-1\text{ mm}$ 的情形, 图 8, 图 9,

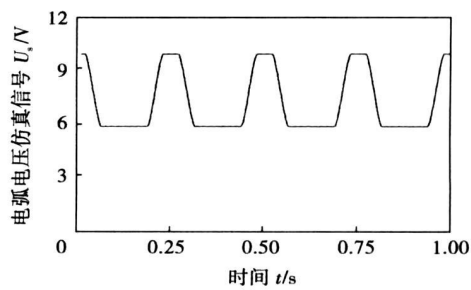


图 8 搭接坡口不对中时系统扫描电压变化波形
Fig. 8 Simulated result of voltage signal for non-midst system

图 10 分别是两种建模得到的仿真波形和实际电弧电压波形。

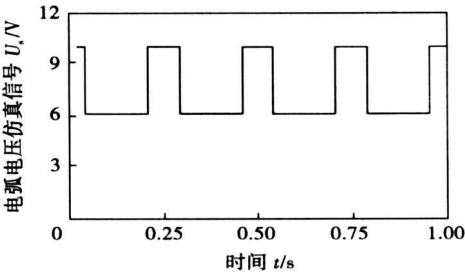


图 9 传统模型系统扫描电压变化波形
Fig. 9 Simulated result of voltage signal for traditional modeling

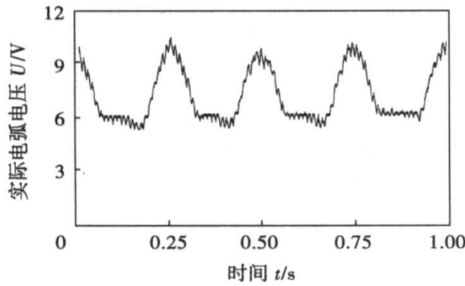


图 10 实际电弧电压波形
Fig. 10 Experimental diagram of arc voltage

比较这三个波形同样可以发现, 文中所建立的仿真模型与传统建模方式所建立的模型相比较, 更为合理, 更符合实际电弧电压波形。

因此, 文中提出建立的 TIG 焊搭接缺口数值仿真模型能有效的提高系统的仿真精度。

3 结 论

- (1) 提出了以焊接电弧圆柱体体积 $V(t)$ 代替传统的扫描坡口的焊枪高度变化信号作为仿真系统输入信号的思路及建模方法。
- (2) 建立了电弧扫描搭接坡口体积变化规律模型, 并由此建立了系统整体仿真模型。
- (3) 通过对模型的仿真分析, 得到了电弧电压的传感信号波形, 并且将此波形与同参数下传统建模仿真计算得到的波形以及同参数下实际电弧电压采样波形进行了对比分析。结果表明, 以电弧电弧圆柱体体积 $V(t)$ 作为仿真系统输入信号建立起来的系统仿真模型的计算结果与实际焊接试验结果基本吻合, 其吻合程度优于传统建模方法得到的仿真波形。

参考文献:

[1] 杨春利, 林三宝. 电弧焊基础[M]. 哈尔滨: 哈尔滨工业大学出版社, 2003.

[2] Christner B K, Lovell R, Campbell M. Developing a GTAW penetration control system for the Titan IV Program[J]. Welding & Metal Fabrication, 1998(4): 33—38.

[3] 陈桂明, 张明照, 戚红雨, 等. 应用 MATLAB 建模与仿真[M]. 北京: 科学出版社, 2003.

[4] 余文松, 薛家祥, 黄石生, 等. CO₂ 焊弧焊动态 MATLAB 仿真研究[J]. 焊接学报, 1999, 20(3): 153—157.

作者简介: 洪 波 男, 1960 年出生, 博士, 教授。主要从事焊接自动化和仿真建模、数值计算等方面的科研和教学工作。发表论文 30 余篇。

Email: hongbo@xtu.edu.cn

Key words: histogram equalization; welding seam; image binarization; edge extraction

The flowing behavior of weld metal in thickness of the plate and the formation mechanism of the onion ring KE Liming^{1,2}, PAN Jiluan¹, XING Li², HUANG Yongde² (1. Key Laboratory for Advanced Materials Processing Technology, Ministry of Education, Tsinghua University, Beijing 100084, China; 2. School of Materials Science and Engineering, Nanchang Hangkong University, Nanchang 330063, China). p39—42

Abstract: The plastic flow behavior of the weld metal during friction stir welding was analyzed by using the multi-plate piled up with several thin copper foils and aluminum sheets and the copper foils serves as a marker material. The results show that there is a serious material translation in the thickness of the weld along the screw thread if using a pin with screw threaded surface. These flowing materials will slough off from the thread at the tip or root of the pin and squeeze into the surrounding area, forming a solid ring with the center being the circle of tip or root of the pin. There is a distinct boundary between the solid ring and its surrounding parent metal. The onion ring is actually the projecting picture of the solid ring cut at the cross section of the weld. The driving force of the metal flow in the thickness of the weld is the pressure of the skew threads on the pin surface to its surrounding plastic metal. When the stir tool rotates clockwise, the center of the onion rings deflect to the bottom of the weld in the case of the pin with left-hand skew thread on its surface, or deflect to the up surface of the weld in the case of the pin with right-hand skew thread on its surface.

Key words: friction stir welding; plastic flow; onion ring

Mathematical modeling and simulation on the lap welding groove of waving TIG HONG Bo, HUANG Mingcan, YIN Li, GONG Hai (Department of Mechanical Engineering, Xiangtan University, Xiangtan 411105, China). p43—46

Abstract: According to the character of the lap joint groove, the signal of the changing bulk of the column as the input signal was introduced into the mathematical model for the waving TIG welding of the lap joint groove, and the simulating model for the whole system accordingly was set up. Keeping the techniques parameters, the differences between the simulating results of this modeling, the traditional results which was made use of changing the height of the welding torch and the welding experiments results were analyzed and compared. It proves that the model reflects the reality, and more accurate than the traditional ones.

Key words: TIG welding; lap welding groove; mathematical modeling and simulation; columned arc

Inspection of fillet weld shape dimension based on laser vision sensing FU Xibin¹, LIN Sanbao¹, YANG Chunli¹, FAN Chenglei¹, QIAN Xia² (1. State Key Laboratory of Advanced Welding

Production Technology, Harbin Institute of Technology, Harbin 150001, China; 2. Department of Industrial Engineering, Binzhou Vocational College, Binzhou 256603, China). p47—50

Abstract: In order to overcome the limitations of fillet weld shape dimension by manual inspection, an inspection method based on laser vision sensing is adopted. Firstly, a laser stripe image is acquired with a laser vision sensor based on principles of optical triangulation. Then the acquired laser stripe image is processed by medium filter, binary processing, laser stripe centerline extraction, and feature recognition algorithms. At last, the information about weld shape dimension is obtained. The experiments show that compared with manual inspection method, the method is much more accurate and reliable to inspect, convenient to use, and the inspection time is greatly shortened, the inspection items are increased obviously, the difference depending on user can be eliminated, and inspection data can be saved in PC.

Key words: laser vision; fillet weld; shape dimension; manual inspection

Effect of Ge on the SnAgCu/Cu soldering interface MENG Gongge¹, YANG Tuoyu², CHEN Leida³, WANG Shizhen¹, LI Caifu⁴ (1. School of Material Science & Engineering, Harbin University of Science and Technology, Harbin 150040, China; 2. Anhui Science and Technology University, Bengbu 233100, China; 3. Dalian University of Technology, Dalian 116024, China; 4. Institute of Metal Research Chinese Academy of Sciences, Shenyang 110016, China). p51—53, 56

Abstract: Germanium (Ge) is adjacent to Tin in periodic Table of the Elements; they are both in the main group IV and resemble each other in physical and chemical properties. A little element Ge was added into lead-free solder Sn2.5Ag0.7Cu (0.25, 0.5, 0.75, 1.0 wt%) and soldering interfaces were made up. The interfacial microstructure and photography were observed and analyzed with scanning electron microscope, the intermetallic compound thickness was measured with Auto CAD software, and interfacial composition was analyzed with energy dispersive X-ray analyzer. The results show that the pattern of IMC layer is pebble shape yet when adding element Ge, but displays a growth trend; the interface gets plainer and more regular with 150 °C/100 h aging. The interfacial IMC layer is thicker with Ge in solder, but the ratio of getting thicker is smaller with 150 °C/100 h aging. The addition of element Ge restrains the transformation of IMC Cu₆Sn₅ to Cu₃Sn and the growth during aging.

Key words: lead-free solder; interface; aging; Ge

Hydrogen dissolving capacity in slag and diffusible hydrogen in deposited metal GUI Chibin, WANG Zheng, WEN Jiancheng (Naval University of Engineering, Wuhan 430033, China). p54—56

Abstract: Effects of composition of the slag on the diffusible hydrogen content in deposited metals were studied by means of changing the content of CaO and MgO in the basic electrode slag and changing the content of Al₂O₃ and MgO in the CO₂ gas-shielded